

# Analyzing the Young's Modulus and Residual Stress of Thin Film MEMS Cantilevers and Bridges Using Static Bending (Oct 2014)

Frankley C. Bwalya, *frankley@mit.edu*, and Yousef S. Alowayed, *Alowayed@mit.edu*, Thursday PM, October 2014

**Abstract**—Thin-film MEMS cantilevers and bridges of various lengths and widths were fabricated using photolithography and wet etching, and were tested using a Hysitron TriboIndenter to deform the cantilevers and bridges. Static deflection data with force measured against the deformation of the devices was collected, and used to calculate the Young's modulus and residual stress of these devices, using the ideal cantilever and small displacement models outlined in this paper. The values of Young's modulus were found to be  $195 \pm 15$  GPa and  $180 \pm 15$  GPa, while the values for residual stress were  $564 \pm 35$  MPa and  $694 \pm 35$  MPa. These values were compared to literature and were within a few standard deviations of those values. A discussion of the effects of fabrication on material properties is presented to explain the discrepancies between the values in literature and the ones calculated in this experiment. However, the findings show that the static bending methods of measurement for thin-film MEMS is a viable option to calculate the physical properties of these films, compared to other methods such as Marco-tensile testing and Electro-Mechanical testing which are more costly and require specific materials to be implemented.

**Index Terms**—Residual Stress, Silicon Nitride, Static Bending, Thin-film MEMS, Wet Etching, Young's Modulus

## I. INTRODUCTION

THE growth of micromachining processing technologies for micro electro-mechanical systems (MEMS) has generated a need for simple, accurate, and standardized means of extracting material property, such as Young's modulus and residual stress in this case, at the micro scale of current MEMS wafers. Knowing these material properties are paramount during the calibration of MEMS that are used in accelerometers, gyroscopes, pressure sensors, microphones, and other devices where the displacement correlated to an applied force must be calculable in advance to provide accurate readings of pressure, spatial orientation, etc [1].

Manuscript received October 22, 2014. This work was supported in part by the Massachusetts Institute of Technology.

F. C. Bwalya is an undergraduate Junior at the Massachusetts Institute of Technology, Cambridge, MA, 02139 USA. (phone: 303-555-5555; e-mail: frankley@mit.edu).

Y. S. Alowayed, is an undergraduate Junior at the Massachusetts Institute of Technology, Cambridge, MA, 02139 USA. (phone: 540-998-8887 e-mail: alowayed@mit.edu).

Existing methods, such as Macroscopic tensile testing have been used to experimentally determine the elastic modulus and failure stress of different materials, including MEMS devices [2]. However, the methods and devices needed are expensive and complex. To compute the mechanical properties of the MEMS, several identical samples must be tested because the samples are permanently deformed during testing, making this method inapplicable to MEMS that are difficult or expensive to manufacture. An alternative to Macroscopic testing methods is Electro-Mechanical testing [3]. This method uses Columbic attraction and variations in capacitance to determine the force and displacement of the devices. Electro-Mechanical testing provides more accurate measurements, but cannot be applied to non-conductive devices.

In this paper we make use of small displacements and static bending techniques, which are cheaper and applicable to a wider range of materials, to calculate the Young's modulus and Residual stress of  $\text{SiN}_x$  MEMS cantilevers and bridges. These values were found to be within a few standard deviations of the values found in literature. The theoretical model, based on the ideal cantilever assumption, is presented and implemented to analyze the data and calculate the Young's modulus and Residual stress in this paper.

## II. EXPERIMENT

### 2.1 Fabrication

Prior to fabrication,  $\text{SiN}_x$  was deposited onto a silicon wafer using low-pressure chemical vapor deposition (LPCVD) to achieve a thin layer of  $\text{SiN}_x$  that will make up the cantilevers and bridges. To fabricate the devices, the wafers were plasma etched using  $\text{SF}_6$  through a mask containing the outline of the cantilevers and bridges. The etched areas were then stripped using oxygen plasma. Wet etching of the exposed silicon substrate, using 20% concentration of KOH at 80 °C, was used to release the cantilevers and bridges. Due to the anisotropic properties of the silicon substrate, the wet etch produced symmetric (111) planes under the cantilevers and bridges, and also resulted in a self terminating wet etch process (figure 1). The self-termination and anisotropic properties of silicon helped to reduce the undercut of our devices while producing a deep groove under the bridges and cantilevers. Alignment of the mask and the crystallographic orientation of the silicon

wafer was carefully monitored throughout the experiment to reduce the undercut of the devices.

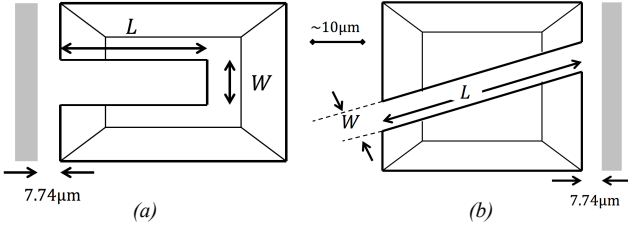


Fig 1. (a) Top view of the cantilever. (b) Top view of the bridge. In each case there is a  $7.74\mu\text{m}$  undercut. The length scales are in the  $10$ 's of  $\mu\text{m}$ .

## 2.2 Testing

The thickness and refractive index of the  $\text{SiN}_x$  were measured using a UV-1280 Thin Film Measurement System. The cantilever and fixed-fixed beams were mechanically tested to determine material and device performance characteristics using a Hysitron TriboIndenter. The Hysitron TriboIndenter was used to apply a vertical force to the cantilevers and bridges (figure 2), using a blunt conical shaped diamond tip with a  $10\mu\text{m}$  radius of curvature and a  $60^\circ$  apex angle, and the corresponding deflection of the cantilevers and bridges was recorded. A conical tip was used because the beams were being deflected instead of indented. Load versus deflection experiments were performed on the  $20 \times 100\mu\text{m}$  cantilever,  $50 \times 100\mu\text{m}$  cantilever and the  $10 \times 50\mu\text{m}$  bridge. A spring constant was calculated from the load versus deflection curves, and used to determine the Young's Modulus of the silicon nitride and residual stress of the bridges.

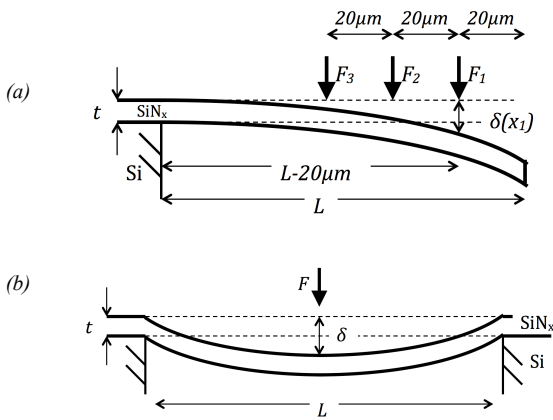


Fig 2. Side view of the cantilever which was displaced at 3 different locations (a), and bridge (b) which was only displaced at the center until breaking.

## III. RESULTS AND DISCUSSION

### 3.1 Cantilevers

To develop the theoretical model for the cantilever, the ideal root cantilever model (no rotation and constant cross section) was assumed [4]. The displacement of the cantilevers due to a

force at a distance  $x$  from the cantilever root is given by:

$$\delta(x) = \frac{FL}{2EI} x^2 \left(1 - \frac{x}{3L}\right) \quad (1)$$

Where,  $E$  is Young's modulus, and  $I$  denotes the second moment of the area of the cross section of the beam around the neutral axis and depends on the geometry of the cross section, as given by:

$$I = Wt^3/12. \quad (2)$$

In our theoretical model, the force  $F$  can be approximated by a spring with constant  $k$ , where  $k = F/\delta(x=L) = 3EI/L^3$  from (1). Combining the equation for  $k$  with (2):

$$E = \frac{4k}{W} \left(\frac{L}{t}\right)^3 \quad (3)$$

$k$  can be found experimentally from the gradient of  $F(\delta)$ . By applying  $F(\delta)$  at various distances of  $x$  from the root of the cantilever, we obtain several  $k$ 's, each associated with a different lengths  $x_i$ , as shown in figure 3.

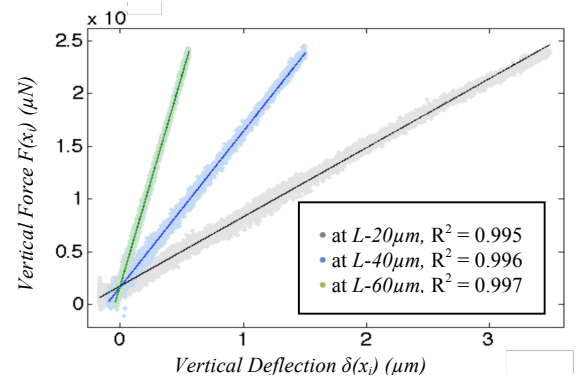


Fig 3. Measured force, plotted against the measured lateral displacement for the  $20 \times 100\mu\text{m}$  cantilever. The grey data points were collected when the force was applied a distance  $x_1 = L - 20\mu\text{m}$  from the root, blue was applied at  $x_2 = L - 40\mu\text{m}$ , and green at  $x_3 = L - 60\mu\text{m}$ . The different gradients of the linear fits of the data are equal to  $k_1, k_2, k_3$ , for each of  $x_1, x_2, x_3$  respectively.

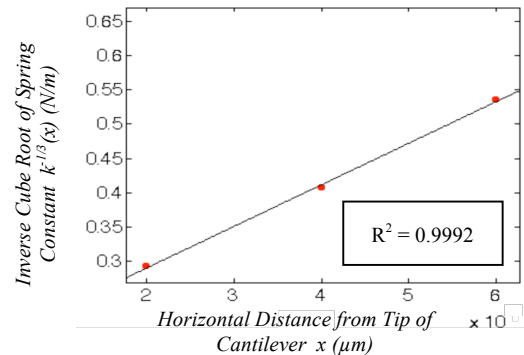


Fig 4. Plot of  $k^{-1/3}$  against  $x \in \{20\mu\text{m}, 40\mu\text{m}, 60\mu\text{m}\}$  for the  $20 \times 100\mu\text{m}$  cantilever. The gradient of the linear fit (black line) is equal to  $(4/EWt^3)^{1/3}$ . Knowing the geometry of the cantilever allows us to then calculate Young's modulus  $E$ .

Plotting  $k_i^{-1/3}$  against  $x_i$  will result in a straight line, as seen in figure 4, with gradient  $dk^{-1/3}/dx = (4/EWt^3)^{1/3}$  from (3), which gives a numerical value for the Young's Modulus  $E=195\pm15\text{GPa}$  for both cantilevers (table 1). The discrepancy between this value and the values found in literature may be a result of measurement inaccuracy, material defects, variations in material structure, etc. It should be noted that values in literature compared to each other differ by several standard deviations. This suggests that the methods of fabrication may play a large role in altering material properties, even when the final materials are chemically and geometrically equivalent. This however may not be the case since the bridge was fabricated on the same wafer and thus should have the same Young's modulus as the cantilevers, which is not the case as will be presented in the next section.

### 3.2 Fixed-fixed bridge

The Young's modulus  $E$  for the  $20\times100\mu\text{m}$  bridge was also calculated by a similar method to the one used for the cantilevers. Force was applied at the center of the bridge, and force against displacement data was measured similar to the cantilevers. The bridge however does not exhibit a linear spring constant similar to the cantilevers due to the two fixed ends, and instead the applied force has a linear and quadratic relation dependence on displacement. Thus bridges requires a more complex model:

$$F = \left( \left( \frac{\pi^2}{2} \right) \left( \frac{\sigma_0 W t}{L} \right) + \left( \frac{\pi^4}{6} \right) \left( \frac{E W t^3}{L^3} \right) \right) \delta + \left( \left( \frac{\pi^4}{8} \right) \left( \frac{E W t^3}{L^3} \right) \right) \delta^3. \quad (4)$$

Plotting  $F/\delta$  against  $\delta^2$ , yields a straight line whose gradient depends on  $E$  and the geometry of the bridge, and whose  $F/\delta$ -axis intercept depends on  $E$ ,  $\sigma_0$ , and the bridge's geometry according to (4) (figure 5).

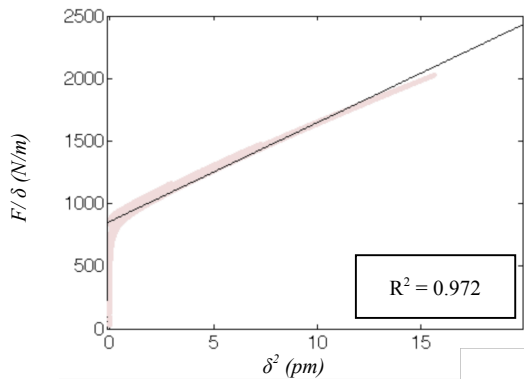


Fig 5. Measured  $F$  and  $\delta$ , plotted as  $F/\delta$  against  $\delta^2$  such that the gradient of the linear fit of the data (black line) will depend only on  $E$  and the geometry of the bridge, and the  $F/\delta$ -axis intercept depends only on  $E$ ,  $\sigma_0$ , and the bridge geometry. This allows easy calculation of  $E$  and  $\sigma_0$ .

The value for the Young's Modulus of the bridge was found to be  $E=180\pm15\text{GPa}$ , which differs from the values found for the cantilevers, although both were fabricated on the same

wafer. This suggests that fabrication methods may not be the dominant source of error. And seeing as the only other sources are measurement and analysis, we may conclude that the method used in this paper, although cheaper and easier than others, may not be as accurate.

The value of  $\sigma_0$  was also calculated and found to be  $564 \pm 35\text{ MPa}$  and  $694 \pm 35\text{ MPa}$  each calculated from data gathered from two separate tests conducted on the bridge. These values for  $\sigma_0$  are high compared to the results in Sekimoto [9], but this may be due to different fabrication methods since  $\sigma_0$  has a greater dependence on fabrication than  $E$ . We are also unable to disprove the effects of fabrication on  $\sigma_0$  because only one bridge was tested. Further investigation is required determining the dominant source of variations in the residual stress.

TABLE I  
AVERAGE VALUES OF  $E$  COMPARED WITH LITERATURE

Source	Value of $E$ (GPa)
20×100μm Cantilever	195 ± 15
50×100μm Cantilever	195 ± 15
10×50μm Bridge	180 ± 15
McShane [5]	155 ± 20
Guo [6]	199 ± 6
MIT Material Database [7]	270 ± NA

## IV. CONCLUSION

To address the growing demand to analyze the physical properties of MEMS devices, this paper has presented and explored a cheap and simple method, utilizing static bending to extract the Young's modulus and residual stress of MEMS cantilevers and bridges. The cantilevers and bridges were fabricated using plasma etching and wet etching with self-terminating properties. The Young's modulus was calculated from static beam bending measurements against the deflection of the cantilever/bridge at different lengths from the root of the cantilever. Discrepancies were found between the value of Young's modulus in literature and the ones calculated in this experiment. The effects of fabrication may be considered minimal because there were variations in the Young's Modulus between the bridge and cantilevers, even though they were fabricated on the same wafer. This suggests that the method presented in this paper, although cheaper and easier than others, may not be as accurate. The residual stress of the bridge was also computed, but was high when compared to the values in literature. This may be due to an error in the theoretical model, or differences in fabrication techniques, but cannot be further investigated in this paper since only one bridge was tested. Further investigation must be made to observe the effects of the parameters of the vapor deposition of  $\text{SiN}_x$  on the residual stress of  $\text{SiN}_x$ .

## REFERENCES

- [1] Mohamed Gad-el-Hak 2001 *The MEMS Handbook* (CRC Press) p 125
- [2] Sharpe W N, Bagdahn J, Jackson K and Coles G 2003 Tensile testing of MEMS materials - recent progress *J. Mater. Sci.* **38** 4075–9

- [3] Osterberg P M and Senturia S D 1997 M-TEST: a test chip for MEMS material property measurement using electrostatically actuated test structures, *J. Microelectromech. Syst.* **6** 107–18
- [4] Crandall S H, Dahl N C and Lardner T J 1972 *Introduction to the Mechanics of Solids* (New York: McGraw-Hill) p 511
- [5] G. J. McShane, M. Boutchich, A. Srikantha Phani, D. F. Moore and T. J. Lu, *J. Micromech. Microeng.*, 2006, 16, 1926
- [6] H. Guo and A. Lal, *Die-Level Characterization of Silicon-Nitride Membrane/Silicon Structures using Resonant Ultrasonic Spectroscopy*, *J. Microelectromech. Syst.*, vol. 12, pp. 53-63, 2003.
- [7] Pierson, Hugh O., *Handbook of chemical vapor deposition (CVD) : principles, technology, and applications*, 2nd edition. Knovel, Ch. 10, pg.281
- [8] G. O. Young, “Synthetic structure of industrial plastics (Book style with paper title and editor),” in *Plastics*, 2nd ed. vol. 3, J. Peters, Ed. New York: McGraw-Hill, 1964, pp. 15–64.
- [9] Misao Sekimoto, Hideo Yoshihara, and Takashi Ohkubo, *Silicon Nitride Single Layer X-Ray Mask*, Musashino Electrical Communication Laboratory, PACS number: 81.15.Gh, 78.65.Jd, 85.40.Ci